Pancreatic cancer is associated with aberrant monocyte function and successive differentiation into macrophages with inferior anti-tumour characteristics

Juusola, Matilda

2021-03

Juusola , M , Kuuliala , K , Kuuliala , A , Mustonen , H , Vähä-Koskela , M , Puolakkainen , P & Seppänen , H 2021 , ' Pancreatic cancer is associated with aberrant monocyte function and successive differentiation into macrophages with inferior anti-tumour characteristics ' , Pancreatology , vol. 21 , no. 2 , pp. 397-405 . https://doi.org/10.1016/j.pan.2020.12.025

http://hdl.handle.net/10138/341580
https://doi.org/10.1016/j.pan.2020.12.025

Pancreatic Cancer is Associated with Aberrant Monocyte Function and Successive Differentiation into Macrophages with Inferior Anti-Tumour Characteristics

Matilda Juusola[1,2], Krista Kuuliala[3], Antti Kuuliala[3], Harri Mustonen[1], Markus Vähä-Koskela[4], Pauli Puolakkainen[1,2], Hanna Seppänen[1,2]

[1]Department of Surgery, [2]Translational Cancer Medicine Research Program, [3]Bacteriology and Immunology, [4]Institute for Molecular Medicine Finland (FIMM), University of Helsinki

Helsinki University Hospital and University of Helsinki

Short Title:

Pancreatic cancer affects monocyte function and differentiation into macrophages

Corresponding author:

Dr. Matilda Juusola

Address: Surgical laboratory, B421b, Biomedicum Helsinki 1

Haartmaninkatu 8, 00290 Helsinki, Finland

Email: matilda.juusola@helsinki.fi

Phone: +358 9 47171827

Fax: --

Abstract:

Background/objectives: Inflammation is related to the development and progression of pancreatic cancer (PC). Locally, anti-inflammatory macrophages (M2), and systemically, high levels of certain inflammation-modulating cytokines associate with poor prognosis in PC. The detailed effects of systemic inflammation on circulating monocytes and macrophage polarisation remain unknown. We aimed to find out how intracellular signalling of peripheral blood monocytes is affected by the systemic inflammatory state in PC patients and how it affects their differentiation into macrophages.

Methods: Monocytes were isolated from 50 consenting PC patients and 20 healthy controls (HC). The phosphorylation status of the signalling molecules was assessed by flow cytometry both from unstimulated and appropriately stimulated monocytes.

Monocytes derived from HC and PC patients were co-cultured with cancer cells (MIA PaCa-2 and HPAF-II) in media supplemented with autologous serum, and the CD marker expression of the obtained macrophages was assessed by flow cytometry.

Results: Phosphorylation levels of unstimulated STAT2, STAT3 and STAT6 were higher ($p<0.05$) and those of stimulated NF-kB ($p=0.004$) and STAT5 ($p=0.006$) were lower in patients than in controls. The expression of CD86, a proinflammatory (M1) marker, was higher in control- than patient-derived co-cultured macrophages ($p=0.029$).

Conclusions: Circulating monocytes from PC patients showed constitutive phosphorylation and weaker response to stimuli, indicating aberrant activation and immune suppression. When co-culturing the patient-derived monocytes with cancer cells, they differentiated into macrophages with reduced levels of M1 macrophage marker CD86, suggesting compromised anti-tumour features. The results highlight the need for global management of tumour-associated immune aberrations in PC treatment.

Key words (max 5):

Immunosuppression

Inflammation

Macrophages

Monocytes

Pancreatic Neoplasms

Introduction:

Inflammation and immune responses have significant, but thus far poorly known, associations with the development and progression of cancer (1). Patients with chronic pancreatitis, for example, have an 8-16-fold risk to develop pancreatic cancer (PC) (2-5). Systemic inflammation is characterized by activation of circulating immune cells and systemic release of inflammatory mediators (6, 7). In patients with cancer, these events can cause symptoms such as weight loss and fatigue and predispose to the development of venous thrombosis (6, 8). The five-year survival in PC is <10%, with shorter survival times associating with systemic inflammation (9, 10). Cancer can also promote inflammation in several ways. Tumour-secreted cytokines, tumour cell necrosis and tumour-caused death of nearby healthy tissue cause local inflammation (11). Cancer-invading immune cells contribute to local inflammation by producing both anti- and pro-inflammatory cytokines (12) and are one key aspect in conferring local responses to systemic inflammation.

One of the first cells to invade inflamed tissues are monocytes. Depending on the profile of inflammatory cytokines in the tissue environment, they differentiate into pro-inflammatory M1 or anti-inflammatory (pro-tumourigenic) M2 macrophages. The number of M2 macrophages has been shown to associate with poor prognosis and higher incidence of lymph node metastasis in PC (13). In co-cultures, M2 macrophages induce an increased migration rate of pancreatic cancer cells (14).

PC patients have elevated levels of circulating inflammatory mediators favouring Th2-oriented immune responses (15). How the cancer-associated immune-inflammatory state affects circulating monocytes, and how broadly this in turn affects their function as macrophages, is still unknown.

Previously, studying patients with non-cancerous systemic inflammation, we have discovered several disease activity- and treatment response-associated biomarkers from circulating leukocytes. These are mostly phosphorylations of crucial signalling proteins, which are likely to be influenced by circulating cytokines (16-20). We have also found that co-culture with PC cells activates the same signalling pathways in macrophages

(14). In the present study we searched for cancer-associated aberrant phosphorylations of the transcription factors nuclear factor (NF)-kB and signal transducers and activators of transcription (STATs), and Akt kinase in circulating monocytes. In addition to their constitutive phosphorylation, response upon stimulation was determined, as a decreased response could refer to immune suppression. We also aimed to reveal how the cancer-associated immune-inflammatory state affects monocyte differentiation into M1 or M2 macrophages as well as migration upon invasion into cancerous tissue.

Materials and Methods:

Patients:

58 patients with suspected PC were enrolled of which eight patients with other histology (cholangiocarcinoma) were excluded. Patients were operated at Helsinki University Hospital between January 2018 and June 2019.

Due to practicalities and as the amount of blood that we could draw per patient was limited, we divided the enrolled 50 PC patients into four different substudies. For the monocyte signalling study, the final number of patients was 23 (16 men, 7 women, aged from 49 to 84, mean 69 years). Monocytes were isolated and cultured from seven patients analysed for macrophage characteristics (3 men, 4 women, aged from 53 to 78, mean 68 years). Monocytes from six patients were used in the migration experiment (4 men, 2 women, aged from 48 to 82, mean 70 years). Serum cytokine expression was assessed from 14 patients (8 men, 7 women, aged from 59 to 82, mean 67 years).

A total of 20 healthy volunteers served as the healthy control (HC) group. Fourteen controls were recruited for the monocyte signalling study (9 women, 5 men, aged from 41 to 86 years, mean 63 years), and the remaining six (5 women, 1 man, aged from 26 to 70, mean 43) were used in the other three substudies. For inclusion, neither the patients nor the controls could have a currently ongoing infection or suffer from any chronic inflammatory disease (such as chronic pancreatitis).

Both the Department of Surgery at Helsinki University Hospital as well as the Surgical Ethical Review Board of the Joint Authority for the Hospital District of Helsinki and Uusimaa approved the study protocol. We obtained informed consent from each patient.

Monocyte signalling

Antibodies

For monocyte surface staining, APC-Cy7-conjugated anti-CD14 antibody (clone HCD14, IgG1 κ) was purchased from BioLegend. For intracellular phosphospecific labeling we used AlexaFluor488-conjugated anti-pSTAT3 (pS727) (clone 49/p-Stat3, IgG1) and anti-pSTAT5 (clone 47/Stat5(pY694), IgG1 κ), AlexaFluor647-conjugated anti-pNF-κB p65 (pS529) (clone K10-895.12.50, BALB/c IgG2b κ), anti-pSTAT1 (pY701) (clone 4a, IgG2a) and anti-pSTAT6 (pY641) (clone 18/P-Stat6, IgG2a), and PE-conjugated anti-pSTAT3 (pY705) (clone 4/P-Stat3, IgG2a), anti-pSTAT4 (pY693) (clone 38/p-Stat4, IgG2b κ) and anti-pAkt (pS473) (clone M89-61, BALB/c IgG1 κ), from Becton Dickinson Biosciences (San Jose, CA, US), and FITC-conjugated anti-pSTAT2 (pY689) (IgG) from Thermo Fisher Scientific. For monocyte HLA-DR determinations we used FITC-conjugated anti-CD14 (clone MϕP9, BALB/c IgG2b κ), PE-conjugated anti-HLA-DR (clone L243, BALB/c IgG2a κ) and its isotype control (mouse IgG2a κ) from Becton Dickinson.

Monocyte-stimulating agents

The recombinant cytokines tumour necrosis factor (TNF), IL-4, IL-6 and interferon (IFN)-γ were from R&D Systems (Minneapolis, MN, US), IFN-α-2a (Roferon) from Roche (Basel, Switzerland) and granulocyte-monocyte colony-stimulating factor (GM-CSF) from Becton Dickinson. Eshcerichia coli 0111:B4 lipopolysaccharide (LPS) was from Sigma (St. Louis, MO, US). The stimulation time and concentration for each agent were optimised in preliminary experiments.

Ex Vivo Stimulation and Immunolabeling of Blood Samples for Three-Color Flow Cytometry:

Just before surgery, a venous blood sample was obtained in an 8.5 ml Vacutainer tube (Becton Dickinson) containing ACD-A (Baxter Health Care Ltd, Norfolk, UK) as anticoagulant and kept at room temperature until the stimulations were started within three hours. The blood sample was divided into eleven 50 µl-aliquots in flow tubes (Beckman Coulter, Brea, CA, US). The tubes were supplemented either with IFN-α 30000 IU/ml (final concentration) for 30 minutes, or IL-6 10 ng/ml, combination of LPS 100 ng/ml and TNF 10 ng/ml or GM-CSF 100 ng/ml and IL-4 10 ng/ml for 10 minutes, or IFN-γ 100 ng/ml for 5 minutes in a 5% CO_2-humidified incubator at +37ºC. Reference tubes were incubated without stimulus. Anti-CD14-APC-Cy7 aliquots were added to all tubes for 15 minutes.

After the incubations, leukocyte fixation, erythrocyte lysis and leukocyte permeabilization were performed according to BD Phosflow Protocol III for Human Whole Blood. Briefly, leukocytes were fixed, and erythrocytes lysed by adding 1 ml of 1x BD Phosflow Lyse/Fix Buffer to each tube and incubating at +37ºC, 5% CO_2 for 10 minutes. After pelleting, leukocytes were washed with BD Pharmingen Stain Buffer and permeabilized by á 0.5 ml of BD Phosflow Perm Buffer III at -20°C for 30 minutes. Cells were pelleted, washed with Stain Buffer and resuspended in á 50 µl of the buffer. Pretitrated amounts of the fluorochrome-labelled phosphospecific Abs were added to the tubes and one unstimulated tube was left without Ab to serve as a background tube. The samples were incubated for 20 min in the dark at room temperature, washed, resuspended in 300 µl of the buffer, stored in the dark on ice, and run on the flow cytometer within three hours.

Monocyte HLA-DR labelling

Upon aliquoting the blood sample, two 25-µl aliquots were pipetted into flow tubes and kept on ice. They were incubated with saturating amounts of anti-HLA-DR- and CD14-FITC Abs in the dark for 20 minutes. Thereafter, erythrocytes were lysed with 1:10 diluted ice-cold FACS Lysing solution (Becton Dickinson) for three minutes on ice, leukocytes were pelleted, and the lysis was completed by repeating the lysing step at room temperature for 5 minutes. Leukocytes were pelleted and resuspended in 300 µl of ice-cold saline supplemented with formaldehyde (final concentration 0.5%) and kept protected from light on ice until performing flow cytometry within four hours.

Phosphospecific flow cytometry

Data acquisition and analysis were done by a CyAn ADP flow cytometer (Beckman Coulter, CA, USA) with FlowJo v10.6 software (Tree Star, OR, USA). Appropriate compensations were performed prior to running the

samples. Monocytes were identified according to their light scattering properties and by creating a CD14-APC-Cy7 fluorescence intensity histogram. AlexaFluor488, FITC, AlexaFluor647 and PE fluorescence histograms were developed from of both unstimulated and stimulated samples and the background tube. The results are presented as the median of relative fluorescence units (RFU, i.e. the geometric mean of the fluorescence channel number). The background fluorescence was subtracted from the unstimulated fluorescence level for each phosphoprotein studied to reveal the actual constitutive phosphorylation levels of the proteins. Fold change, i.e. the fluorescence level of a phosphoprotein in the stimulated sample divided by the corresponding level in the unstimulated sample, was used to illustrate the magnitude of the phosphorylation response of the protein to a given stimulus.

Flow cytometric HLA-DR determination

The proportion of HLA-DR-positive monocytes was determined as follows. Firstly, PE histogram of CD14-FITC positive monocytes was developed using the sample stained with the isotype control antibody. A marker was set to exclude 95–97% of the events, thereby indicating the upper limit of non-specific fluorescence intensity of monocytes. Next, the respective HLA-DR-PE histogram was created, and the proportion of positively fluorescing monocytes was recorded.

Macrophage cultures and characterisation

Cell Cultures and Reagents:

Mononuclear cells were isolated from PC patients' and healthy subjects' blood by density gradient centrifugation (Ficoll-Paque, Amershamn, Uppsala, Sweden). We used magnetic beads to separate monocytes (Human Monocyte Isolation kit II from Miltenyi Biotec, Auburn, USA). Blood samples from different individuals were processed separately. Monocytes from the same donor were treated as internal controls in each of the study settings.

The pancreatic adenocarcinoma cell lines used were MIA PaCa-2 (primary tumour) and HPAF-II (metastatic cell line) from the American Type Culture Collection. For culture, we used the media recommended in the product sheet (DMEM with 10% FBS for MIA PaCa-2, and EMEM with 10% FBS, 2.5% Horse serum for HPAF-II). Patient- and control-derived monocytes were matured into macrophages in Macrophage Serum-free Media (Gibco Life Technologies, Paislay, UK) supplemented with penicillin (Sigma, St.Louis, USA) 100 mg/ml and

15% autologous serum. After five days, MIA PaCa-2 and HPAF-II cells were added to the cultures. The macrophage:cancer cell ratio was 1 million:300 000 per well. Cells were seeded on Thermo Fisher Nunc™ Dishes with UpCell™ Surface (21.5 cm^2) to ease detaching. After two days of co-culture, the cells were detached by a 20-minute incubation at room temperature, collected in PBS and filtrated. Macrophages were labelled with selected antibodies for 20 minutes at room temperature.

Macrophage Characterisation:

The surface marker antibodies used were Mouse Anti-Human CD14-FITC, CD86-PE and -APC, CD163-PE, CD209-APC, CD204-PE, with respectively fluorochrome-conjugated Mouse IgG1 κ Isotype Controls (BD Pharmingen, San Diego, USA). Monocytes were characterized as a start point control. Characterisation was acquired on FACS Calibur (CellQuest Pro software; BD Bioscience) flow cytometer and data was analysed with WinMDI software (v2.8). We measured CD marker expression (RFU) of macrophages. Macrophages were distinguished from cancer cells by their CD14 positivity.

Cancer Cell Migration Study:

Cells were cultured on 8-well coverslip dishes (Nunc, Thermo Scientific, Rochester, USA) coated with 60 µl Matrigel (BD Biosciences, San Jose, USA). The monocytes were first differentiated into macrophages on Matrigel in media containing 15% autologous serum. After five days of culture, MIA PaCa-2 and HPAF-II cells, which were stained with fluorescent dye (CellTracker Green CMFDA, Invitrogen, Eugene, USA), were added to the culture. Cells were left to settle in a standard cell incubator for 24 hours before microscopy.
Cancer cell migration on Matrigel was assessed by recording stained cell movement with 30-minute intervals for 24 hours under fluorescence microscope (11, 21). We analysed the data using ImagePro software (v 7.01, Media Cybernetics, Rockville, MD, USA). Stained cancer cells were observed with and without the presence of differentiated macrophages.

Cytokine Array:

Cytokine levels in patients' and healthy controls' serum were assessed by a customized, pre-coated human cytokine Q-Plex™ Array (Biosciences) according to the manufacturer's instructions. The sera were diluted 1:2 and loaded to the Q-Plex Array plate. The plate was put on a shaker for two hours at RT. The wells were washed, and Detection Mix was added and incubated again for two hours on the shaker. DyLight IR dye was added and incubated for 30 minutes on the shaker until Stabilizing solution was added, and the plate was dried

by centrifuging (300G, 5 minutes) and air drying for 30 minutes at RT. The array was imaged with the Odyssey infrared imager (Licor Biosciences, Lincoln, NE, USA) and dot blots were analyzed densitometrically with Odyssey software (Licor Biosciences). The detected cytokines were IFN-γ, IL-1α, IL-1b, IL-1ra, IL-6, IL-8, IL-10, and IL-23, MCP, RANTES and TNF.

Statistical analysis:

For non-normally distributed data, including cytokine profiles as well as macrophage CD markers, the Mann-Whitney test was used to compare groups. A two-way Student's t-test was used to assess cancer cell migration in co-culture settings.

Correlation coefficients were calculated using the Spearman method and the Jonckheere-Terpstra test was used to assess trends. In multiple comparisons, the Benjamini-Hochberg Procedure was used to adjust for false discoveries (false discovery rate set to 5%), and adjusted p-values were computed by the p.adjust function in R. A p-value less than 0.05 was considered significant and two tailed tests were used. SPSS version 24.0 (SPSS, Inc., Chicago, IL, USA), and R version 3.6.1 (Foundation for Statistical Computing, Vienna, Austria), and STATA/MP (v. 15.1, StataCorp LLC, College Station, TX, USA) were used for statistical calculations.

Results:

Monocyte signalling

Signalling profiles of monocytes in patients with PC vs. healthy controls (HC)

To assess how the systemic inflammatory state in PC patients affects the peripheral blood monocytes we looked at the phosphorylation levels of intracellular signalling molecules. The constitutive phosphorylation levels of

STAT1 (pY701), STAT2 (pY689), STAT3 (pS727 and pY705), and STAT6 (pY641) were significantly higher in patients than in controls (Table 1). Constitutive phosphorylation of STAT4 (pY693), STAT5 (pY694), Akt (pS473), and NF-kB (pS529) did not differ between patients and controls (Table 1).
Next, we wanted to find out was how the monocytes respond to extracellular stimuli. When stimulating the monocytes with relevant stimuli, the fold change of STAT5 and NF-kB phosphorylation was significantly lower in patients than in controls (Table 1). There was no fold change difference in pSTAT1, pSTAT3, pSTAT6 or pAkt levels (Table 1) between patients and controls. In our experimental setting, we obtained no response to IFN-α and so only constitutive phosphorylation levels are given for STAT2 and STAT4.

Low HLA-DR expression in monocytes is associated with immune suppression. In our experiment, we found that HLA-DR expression was, indeed, lower in patients (mean 87%, 95% CI 82% to 90%) than in controls (mean 96%, 95% CI 93% to 97%, p=0.001) (Supplementary figure S1). Together these results indicate a continuous signalling activation causing a possible signalling exhaustion and subsequently reduced ability to react to external stimuli as well as suppression of monocyte immunity. Next we examined how the signalling protein phosphorylation of whole blood monocytes associated with other known prognostic factors in PC.

Table 1.

Molecule	Stimulation	Patients Mean (95% CI)	Controls Mean (95% CI)	p
pSTAT1	Constitutive	1.06 (1.00 - 1.12)	0.96 (0.92 - 1.01)	**0.031**
	IL-6	1.35 (1.25 - 1.47)	1.40 (1.30 - 1.50)	0.70
	IFN-γ	3.04 (2.65 - 3.55)	3.05 (2.58 - 3.63)	0.99
pSTAT2	Constitutive	4.36 (3.99 - 4.74)	3.67 (3.21 - 4.13)	**0.031**
pSTAT3 (pS727)	Constitutive	2.13 (1.92 - 2.35)	1.83 (1.65 - 2.04)	**0.031**
	IL-6	2.32 (2.15 - 2.52)	2.44 (2.26 - 2.67)	0.37
pSTAT3 (pY705)	Constitutive	1.86 (1.73 - 2.07)	1.47 (1.33 - 1.64)	**<0.001**
	IL-6	5.7 (5.30 - 6.21)	5.86 (5.12 - 6.72)	0.97
pSTAT4	Constitutive	1.66 (1.58 - 1.75)	1.56 (1.40 - 1.74)	0.20
pSTAT5	Constitutive	2.97 (2.73 - 3.28)	2.64 (2.33 - 2.94)	0.088
	GM-CSF + IL-4	5.10 (4.75 - 5.46)	5.95 (5.46 - 6.47)	**0.006**
pSTAT6	Constitutive	1.01 (0.96 - 1.06)	0.91 (0.86 - 0.96)	**0.018**
	GM-CSF + IL-4	1.35 (1.25 - 1.47)	1.40 (1.30 - 1.50)	0.19
pNF-κB	Constitutive	1.25 (1.18 - 1.32)	1.16 (1.08 - 1.23)	0.32
	TNF + LPS	2.31 (2.13 - 2.51)	2.83 (2.59 - 3.09)	**0.004**
pAkt	Constitutive	1.99 (1.81 - 2.18)	2.00 (1.69 - 2.32)	0.90
	TNF + LPS	2.04 (1.93 - 2.19)	2.17 (2.00 - 2.43)	0.28

Fold change of signalling markers in unstimulated and stimulated (stimulation agent specified in second column) monocytes.

Serum biomarkers CA19-9 and CEA

Carbohydrate antigen (CA)19-9 ~~levels~~ showed a positive correlation with constitutive STAT2 (r=0.61, p=0.002) and STAT5 (r=0.49, p=0.023) phosphorylation levels, and a negative correlation with IFN-γ -induced STAT1 phosphorylation (r=-0.48, p=0.026) levels (Supplementary table 2). Carcinoembryogenic antigen (CEA) level did not correlate with the phosphorylation levels (Supplementary table 2).

Stage of PC

Of the total of 23 patients, the tumour stage was IV in six, III in eight, IIB in six, and IB in two patients. One patient could not proceed to surgery due to poor general condition, and stage could therefore not be obtained. Owing to the low number of patients with stage IB they were excluded from the analyses.

While constitutive STAT1 and STAT5 phosphorylation associated with higher levels of CA19-9, no stage-associated trend was found in the constitutive phosphorylation levels of these markers ($p>0.05$). However, upon stimulation, the fold increase of STAT1 and STAT5 phosphorylation showed a monotone decreasing trend with increasing stage of PC ($p=0.030$ and $p=0.032$, figure 2), portraying that a compromised capacity to react to stimuli was associated with worse disease stage.

Neither fold change nor constitutive phosphorylation level associated with stage in STAT3, STAT4, STAT6, Akt or NF-kB ($p>0.05$)

Macrophage cultures

Surface markers:

In addition to the phosphorylation of intracellular signalling proteins in monocytes, we wanted to assess how the inflammatory state in PC affects monocyte differentiation into M1 or M2 macrophages in co-culture with cancer cells. We chose to use autologous serum in the culture media in order not to deliberately direct the macrophages to any phenotype (as compared to when using GM-CSF, M-CSF etc.).

The co-culture with cancer cells (MIA Paca-2 and HPAF-II) significantly increased the expression of CD86 ($p<0.001$) (M1 marker) and CD209 ($p=0.022$) (M2 marker) in all culture conditions (Figure 3).

While these markers were increased in both patient ($p=0.010$ and $p=0.046$) and HC ($p=0.035$ and $p=0.046$) derived macrophages (figure 4), the expression of CD86 (M1 marker) increased more in HC than patient derived macrophages ($p=0.046$) (figure 4). A significant increase of CD163 (M2 marker) was seen only in HC derived

macrophages (p=0.010, figure 4). The difference between patient and control was, however, not statistically significant (p=1.000).

No difference was found in the initial expression of CD markers in patient derived monocytes and monocytes drawn from HC (supplementary table 1).

Looking at the two different cancer cell lines separately, we could see a difference between the effect of MIA Paca-2 and HPAF-II on polarization of macrophages. In patient derived macrophages, MIA Paca-2 cells significantly increased the expression of CD86 (p=0.035). HPAF-II cells, in turn, significantly increased the expression of both CD86 (p=0.035) and CD209 (p=0.046, figure 4).

A comparable observation was done in HC derived macrophages co-culture with MIA Paca-2 led to an increase only in CD86 expression (p=0.046). HPAF-II increased the expression of CD86 (p=0.035), and the increase in CD209 was borderline insignificant (p=0.055) (figure 4).

The difference in how the cell lines increased expression of CD86 and CD209 – HPAF-II increasing the expression more – was significant (p=0.046 and p=0.046). When considering the patient derived condition separately, the difference in how MIA Paca-2 and HPAF-II affected CD209 remained (p=0.046), while the difference in CD86 was nonsignificant (p=0.066). In control conditions, the difference in macrophage polarization induced either by MiaPaca-2 or HPAF-II did not vary (p>0.05).

When looking at the three culture conditions as a trend – i.e. macrophages cultured alone, with a cell line derived from a primary tumour site (MIA Paca-2) and finally with a metastatic cell line (HPAF-II), an increasing trend was observed in both PC patient and HC serum conditions in CD86 (p<0.001, and p=0.001, respectively) and CD209 (p=0.025 and p=0.015, respectively) marker expression.

Migration:

Next, we aimed to assess how the differences in polarisation affected the function of macrophages. To do this, we set up an experiment measuring migration. The presence of macrophages increased the migration of cancer cells in serum-supplemented media (p<0.001, Figure 5). However, no significant difference was found between patients and controls with respect to increased migration rate (p=0.259).

Cytokine measurements

Finally, we looked at the serum expression of 11 different cytokines in patient and HC serum. Patient-derived serum was significantly richer in IL-1b (p=0.041), IL-6 (p=0.041), IL-10 (p=0.002), TNF (p=0.003) and Rantes (p=0.005). Patient sera seemed to be richer in IL-1ra, but the difference was only borderline significant (p=0.051). There was no significant difference in IFN-γ, MCP-1, IL-1a, IL-8, and IL-23 concentrations in patient and control sera. (Table 2).

Table 2.

Cytokine	Patient Median (IQR)	Control Median (IQR)	p=
IFN-y	1.59 (0.96)	1.22 (0.67)	0.397
IL-1α	1.96 (14.58)	0.59 (1.92)	0.312
IL-1b	18.65 (22.6)	8.75 (0.00)	**0.041**
IL-1ra	55.33 (68.04)	34.73 (14.72)	0.051
IL-6	3.32 (1.51)	2.21 (0.82)	**0.041**
IL-8	3.28 (2.73)	3.28 (0.00)	0.659
IL-10	12.21 (7.79)	4.57 (0.00)	**0.002**
IL-23	58.45 (40.81)	47.91 (53.28)	0.750
MCP-1	68.54 (41.22)	71.38 (19.92)	0.602
RANTES	1868.90 (917.57)	1182.10 (580.30)	**0.005**
TNF	15.41 (9.05)	6.89 (0.74)	**0.003**

Cytokines in patient and control sera (pg/ml). Serum levels of IL-1b, IL-6, IL-10, TNF and RANTES were higher in patients than healthy controls.

Figure Legends:

Figure 1.

Flowchart of patient enrolment. A total of 58 patients were enrolled, while 8 patients were excluded based on diagnosis other than pancreatic cancer. The final 50 patients were dispersed in the 4 substudies.

Figure 2.

Box and whisker plot showing median, 25%, 75% and range of fold increase in A. STAT1 in monocytes upon IFN- γ stimulation B. STAT5 in monocytes upon GM-CSF+IL-4 stimulation with pancreatic cancer disease stages II, III and IV considered separately. A monotone decreasing trend is seen with increasing disease stage in both markers.

Figure 3.

Box and whisker plot showing median, 25%, 75% and range of CD markers on macrophages either cultured alone or together with cancer cells (MIA Paca-2 and HPAF-II pooled together). *$p<0.05$, ***$p<0.001$. Co-culture with cancer cells increases the macrophage expression of CD86 and CD209.

Figure 4.

Box and whisker plot showing median, 25%, 75% and range of CD markers on patient and healthy control derived macrophages cultured either alone or together with cancer cells (MIA PaCa-2 or HPAF-II). Co-culture with cancer cells increased CD86 and CD209 expression in both patient and control derived macrophages, while CD163 expression increased only in control derived macrophages. The expression of CD86 increased more in control than in patient derived macrophages when co-cultured with cancer cells. Number of comparisons was 10, false discovery rate correction was used. *$p<0.05$.

Figure 5.

Migration speed of cancer cells (MIA Paca-2 and HPAF-II) increased in presence of either patient-derived or control-derived macrophages. Both patient and control derived macrophages increased the migration in a similar manner. ***$p<0.001$.

Discussion:

The results show for the first time that the systemic inflammatory nature of PC is reflected in aberrations in the signalling profile of circulating monocytes, concerning phosphorylated (p) STAT1, -2, -3, -5, -6 and NF-□B, and that the stage of PC is associated with STAT5 and STAT1 signalling. Furthermore, once co-cultured with cancer cells, PC patient -derived monocytes differentiate into macrophages with reduced M1 macrophage marker CD86 expression, suggesting inferior anti-tumour characteristics when compared to HC monocytes.

Our previous findings suggest that constitutively phosphorylated STAT3 in circulating leukocytes is characteristic of systemic inflammatory conditions such as acute pancreatitis, sepsis and early untreated rheumatoid arthritis (18-21). These high pSTAT3 levels may result from systemic STAT3-activating cytokines. Indeed, two of these cytokines, IL-6 and IL-10, were elevated in the serum of PC patients in the present study. In PC cells, IL-6/STAT3 signalling mediates proinvasive effects (22) and have also been shown to release proinflammatory metabolites that favour the accumulation of myeloid-derived suppressor cells (MDSCs). The functions of monocytic MDSCs are orchestrated by STAT3 activation (23). Also, tumour-derived microvesicles may carry bioactive cargo which induces CD44-mediated STAT3 activation in monocytes (24).

As IL-4 is the main activator of STAT6 signalling, the elevated STAT6 phosphorylation in patient monocytes may be due to elevated plasma IL-4 levels. Such have been observed in PC patients in another study (25). IL-4/STAT6 signalling represents the putative Th2 and suppressive immune responses in PC. Furthermore, it has been reported that in patients with resectable PC, simultaneous expression of low IL-4 and high TNF identified patients with best prognosis (26). Also, the magnitude of TNF- and lipopolysaccharide-induced NF-kB phosphorylation was significantly lower in patient monocytes, suggesting a weakening of proinflammatory capacity.

The constitutive STAT1 phosphorylation in patient monocytes in the present study suggests that proinflammatory and Th1-oriented immune responses may also take place simultaneously with the Th2-oriented

ones. High plasma levels of the classical STAT1-activating cytokine IFN-γ are associated with PC (25), but in the present study the IFN-γ levels in patient samples were not significantly higher when compared to HC. However, the calcineurin B subunit, the roles of which are just emerging, has been shown to bind to integrin CD11b on macrophage surface and phosphorylate STAT1 synergistically with IFN-γ (27). Interestingly, CD11b is characteristic of monocytic MDSCs (28, 23), and its density has been reported to increase during differentiation of classical monocytes into metastasis-associated macrophages in a mouse model of metastatic breast cancer (29). Another possibility is that the pSTAT1 levels are elevated due to elevated plasma levels of IL-29 (IFN-lambda), particularly as this cytokine is able to cause phosphorylation of both STAT1 and STAT2, and constitutive phosphorylation of STAT2 was also higher in monocytes of PC patients than in those of HC in the present study. IL-29 is a novel cytokine known to exert anti-tumour effects, and concerning non-small cell lung cancer, high plasma levels of IL-29 have been associated with better overall survival (28).

When studying if the stage of PC is reflected to the monocyte signalling results we found, first, that the magnitude of monocyte STAT1 phosphorylation in response to IFN-γ showed a monotone decreasing trend from patients with tumour stage II to stage IV. This probably reflects weakening of proinflammatory abilities with progression of the disease. IFN-γ is critical not only in the defence against infections but also in tumour surveillance (30-31). IFN-γ -induced STAT1 activation mediates, for example, IL-12p70 release and simultaneous inhibition of IL-10 synthesis in antigen-presenting cells (32). IL-12-activated T lymphocytes further produce high levels of IFN-γ, which is able to modulate the genetic programs of tumour cells so that growth and angiogenesis are inhibited, as shown in carcinoma cell lines (33). Also, in natural killer/T cell lymphoma in mice, inhibition of tumour progression is likely to involve IFN-γ/STAT1 signalling (34).

The magnitude of STAT5 phosphorylation in response to GM-CSF also showed a monotone decreasing trend from patients with tumour stage II to stage IV. Huen et al. found that GM-CSF -induced STAT5 activation in monocytes mediates the development of alternatively activated macrophages with a reparative phenotype different from the “conventional” alternatively activated M2 type favouring tumour progression (35). Interestingly, GM-CSF administration to monocytes of carcinoma patients has been shown to up-regulate phagocytosis of apoptotic tumour cells as well as antigen presentation (36).

CA19-9 (carbohydrate antigen) is currently the only guideline-recommended biomarker for PC; high serum CA19-9 levels are associated with worse outcomes (37-38). We found that serum CA19-9 level showed a positive correlation with constitutive pSTAT2 and STAT5 levels and a negative correlation with IFN-γ -stimulated pSTAT1 level in the patients' monocytes. It has been observed in mice that CA19-9 expression results in hyperactivation of epidermal growth factor receptor (EGFR) signalling (39), and human natural killer cells in which STAT5 is activated via EGFR and IL-15 signalling have been reported to show increased IFN-γ production and cytotoxicity towards cancer cells (40). Apparently, CA19-9 may also contribute to some anticancer functions, and our results highlight the complexity of the network composed of mediators and signalling pathways associated with cancer.

Monocytes from PC patients are inclined to favour anti-inflammatory behaviour in tissue. The co-culture of macrophages with cancer cells (MIA Paca-2 or HPAF-II) led to a lower expression of the proinflammatory marker CD86 in patient derived macrophages as compared to macrophages drawn from HC. Interestingly, it seems that the metastatic cell line HPAF-II was able to increase CD86 expression more than the local PC cell line MIA Paca-2. The expression of CD86 is a good prognostic factor, and induction of CD86, along with other M1 phenotype markers, in macrophages promotes anti-tumour effects (41-43). Our result may be due to an inherited anti-inflammatory profile of monocytes, or to mediators present in the serum. Either way, the experiment showed that patient monocytes are less prone to anti-tumour differentiation when in a milieu representing chronic inflammation. In patient tumour samples, a comparable result of reduced local M1 signalling/increased M2 profile of tumour-infiltrating macrophages is associated with worse prognosis (43-44).

It came as no surprise that serum cytokines were elevated in patient sera. Altogether, of the 11 circulating cytokines we compared between PC patients and HC, tumour necrosis factor (TNF) and the interleukins IL-1b, -6 and -10 were elevated. TNF is commonly elevated in PC and associated with increased cellular growth (45). The proinflammatory IL-1 is a marker for necrosis or tissue damage, IL-6 is commonly elevated in chronic inflammatory diseases and cancer, and IL-10 is pivotal in anti-inflammatory and immunosuppressive functions (46).

It has been known for long that an exaggerated systemic inflammatory response is followed or overlapped by an anti-inflammatory compensation, immune suppression. This predisposes the patient to secondary infections and

death (47, 21). Similarly, chronic immune responses that fail to be terminated by normal feedback mechanisms predispose patients to immune suppression and provides a tumour-supporting microenvironment (48). Our results show that the inflammation not only affects the local deregulation of immune cells, but also causes circulating monocytes to react aberrantly. The continuous inflammatory state may exhaust the monocytes and decrease their reactivity. HLA-DR expression on monocytes was slightly but statistically significantly lower in patients than in HC, supporting a skew towards an immunosuppressive state in the patients' responses (49).

The present study was not able to show differences in migration induction between patient- and control-derived macrophages. It is, however, generally accepted that macrophage polarisation affects the prognosis of PC. The functional mechanisms behind this were therefore outside the study scope. With a relatively small study size, we were nevertheless able to find intriguing differences between patient and control monocyte differentiation into macrophages.

Our current results emphasize the need to recognise and influence the tumour-associated aberrations in local and systemic immune responses such as i) anti-inflammatory macrophage differentiation, ii) monocyte functions showing features immune suppression, and iii) imbalance of circulating cytokines. The signalling aberrations of circulating leukocytes may provide a non-invasive mean to screen the severity of PC. Moreover, the current understanding is that cancer treatment should involve retargeting local immune cells to stop the immune escape of cancer cells. However, to ensure that circulating immune cells take anti-tumour measures once they invade the tumour tissue, tumour-induced immune aberrations should be battled at systemic level.

Acknowledgements:

The authors thank Mrs. Sanna Vainionpää for excellent technical assistance. We also thank the Finnish State Subsidy Fund, Sigrid Jusélius Foundation, Mary and Georg C. Ehrnrooths Foundation, and Finska Läkaresällskapet for funding the study. The author(s) declare no conflicts of interest with respect to the research, authorship, and/or publication of this article.

References

1. Elinav E, Nowarski R, Thaiss CA, Hu B, Jin C, Flavell RA. Inflammation-induced cancer: crosstalk between tumours, immune cells and microorganisms. Nat Rev Cancer. 2013 Nov;13(11):759-71.
2. Lowenfels AB, Maisonneuve P, Cavallini G, Ammann RW, Lankisch PG, Andersen JR, et al. Pancreatitis and the risk of pancreatic cancer. International Pancreatitis Study Group. N Engl J Med. 1993 May 20;328(20):1433-7.
3. Ekbom A, McLaughlin JK, Karlsson BM, Nyren O, Gridley G, Adami HO, et al. Pancreatitis and pancreatic cancer: a population-based study. J Natl Cancer Inst. 1994 Apr 20;86(8):625-7.
4. Kirkegard J, Mortensen FV, Cronin-Fenton D. Chronic Pancreatitis and Pancreatic Cancer Risk: A Systematic Review and Meta-analysis. Am J Gastroenterol. 2017 Sep;112(9):1366-72.
5. Korpela T, Udd M, Mustonen H, Ristimäki A, Haglund C, Seppänen H, et al. Association between chronic pancreatitis and pancreatic cancer: A 10-year retrospective study of endoscopically treated and surgical patients. Int J Cancer. 2020 03/12; 2020/05;n/a.
6. Roxburgh CS, McMillan DC. Cancer and systemic inflammation: treat the tumour and treat the host. Br J Cancer. 2014 Mar 18;110(6):1409-12.
7. Zotova NV, Chereshnev VA, Gusev EY. Systemic Inflammation: Methodological Approaches to Identification of the Common Pathological Process. PLoS One. 2016 May 6;11(5):e0155138.
8. Date K, Ettelaie C, Maraveyas A. Tissue factor-bearing microparticles and inflammation: a potential mechanism for the development of venous thromboembolism in cancer. J Thromb Haemost. 2017 12/01; 2020/01;15(12):2289-99.
9. Salmiheimo A, Mustonen H, Stenman UH, Puolakkainen P, Kemppainen E, Seppänen H, et al. Systemic Inflammatory Response and Elevated Tumour Markers Predict Worse Survival in Resectable Pancreatic Ductal Adenocarcinoma. PLoS One. 2016 Sep 15;11(9):e0163064.

10. Stevens L, Pathak S, Nunes QM, Pandanaboyana S, Macutkiewicz C, Smart N, et al. Prognostic significance of pre-operative C-reactive protein and the neutrophil-lymphocyte ratio in resectable pancreatic cancer: a systematic review. HPB (Oxford). 2015 Apr;17(4):285-91.
11. Munn LL. Cancer and inflammation. WIREs Syst Biol Med. 2017 03/01; 2020/01;9(2):e1370.
12. Diakos CI, Charles KA, McMillan DC, Clarke SJ. Cancer-related inflammation and treatment effectiveness. Lancet Oncol. 2014 Oct;15(11):e493-503.
13. Kurahara H, Shinchi H, Mataki Y, Maemura K, Noma H, Kubo F, et al. Significance of M2-polarized tumor-associated macrophage in pancreatic cancer. J Surg Res. 2011 May 15;167(2):e211-9.
14. Salmiheimo A, Mustonen H, Vainionpää S, Shen Z, Kemppainen E, Puolakkainen P, et al. Tumour-associated macrophages activate migration and STAT3 in pancreatic ductal adenocarcinoma cells in co-cultures. Pancreatology. 2017 Jul - Aug;17(4):635-41.
15. Bellone G, Turletti A, Artusio E, Mareschi K, Carbone A, Tibaudi D, et al. Tumor-associated transforming growth factor-beta and interleukin-10 contribute to a systemic Th2 immune phenotype in pancreatic carcinoma patients. Am J Pathol. 1999 Aug;155(2):537-47.
16. Kuuliala K, Kuuliala A, Koivuniemi R, Oksanen S, Hamalainen M, Moilanen E, et al. Constitutive STAT3 Phosphorylation in Circulating CD4+ T Lymphocytes Associates with Disease Activity and Treatment Response in Recent-Onset Rheumatoid Arthritis. PLoS One. 2015 Sep 9;10(9):e0137385.
17. Kuuliala K, Penttila AK, Kaukonen KM, Mustonen H, Kuuliala A, Oiva J, et al. Signalling Profiles of Blood Leucocytes in Sepsis and in Acute Pancreatitis in Relation to Disease Severity. Scand J Immunol. 2018 Feb;87(2):88-98.
18. Kuuliala K, Kuuliala A, Koivuniemi R, Kautiainen H, Repo H, Leirisalo-Repo M. STAT6 and STAT1 Pathway Activation in Circulating Lymphocytes and Monocytes as Predictor of Treatment Response in Rheumatoid Arthritis. PLoS One. 2016 Dec 12;11(12):e0167975.
19. Oiva J, Mustonen H, Kylanpaa ML, Kuuliala K, Siitonen S, Kemppainen E, et al. Patients with acute pancreatitis complicated by organ dysfunction show abnormal peripheral blood polymorphonuclear leukocyte signaling. Pancreatology. 2013 Mar-Apr;13(2):118-24.

20. Oiva J, Mustonen H, Kylänpää ML, Kyhälä L, Kuuliala K, Siitonen S, et al. Acute pancreatitis with organ dysfunction associates with abnormal blood lymphocyte signaling: controlled laboratory study. Crit Care. 2010;14(6):R207.
21. Shen Z, Kauttu T, Seppänen H, Vainionpää S, Ye Y, Wang S, et al. Both macrophages and hypoxia play critical role in regulating invasion of gastric cancer in vitro. Acta Oncol. 2013 May;52(4):852-60.
22. Razidlo GL, Burton KM, McNiven MA. Interleukin-6 promotes pancreatic cancer cell migration by rapidly activating the small GTPase CDC42. J Biol Chem. 2018 Jul 13;293(28):11143-53.
23. Trovato R, Fiore A, Sartori S, Cane S, Giugno R, Cascione L, et al. Immunosuppression by monocytic myeloid-derived suppressor cells in patients with pancreatic ductal carcinoma is orchestrated by STAT3. J Immunother Cancer. 2019 Sep 18;7(1):255,019-0734-6.
24. Baj-Krzyworzeka M, Weglarczyk K, Szatanek R, Mytar B, Baran J, Siedlar M. The role of CD44H molecule in the interactions between human monocytes and pancreatic adenocarcinoma-derived microvesicles. Folia Histochem Cytobiol. 2019;57(1):28-34.
25. Yako YY, Brand M, Smith M, Kruger D. Inflammatory cytokines and angiogenic factors as potential biomarkers in South African pancreatic ductal adenocarcinoma patients: A preliminary report. Pancreatology. 2017 May - Jun;17(3):438-44.
26. Piro G, Simionato F, Carbone C, Frizziero M, Malleo G, Zanini S, et al. A circulating TH2 cytokines profile predicts survival in patients with resectable pancreatic adenocarcinoma. Oncoimmunology. 2017 Apr 28;6(9):e1322242.
27. Su Z, Yang R, Zhang W, Xu L, Zhong Y, Yin Y, et al. The synergistic interaction between the calcineurin B subunit and IFN-gamma enhances macrophage antitumor activity. Cell Death Dis. 2015 May 7;6:e1740.
28. Barrera L, Montes-Servin E, Hernandez-Martinez JM, Orozco-Morales M, Montes-Servin E, Michel-Tello D, et al. Levels of peripheral blood polymorphonuclear myeloid-derived suppressor cells and selected cytokines are potentially prognostic of disease progression for patients with non-small cell lung cancer. Cancer Immunol Immunother. 2018 Sep;67(9):1393-406.
29. Kitamura T, Doughty-Shenton D, Cassetta L, Fragkogianni S, Brownlie D, Kato Y, et al. Monocytes Differentiate to Immune Suppressive Precursors of Metastasis-Associated Macrophages in Mouse Models of Metastatic Breast Cancer. Front Immunol. 2018 Jan 17;8:2004.

30. Peng W, Liu C, Xu C, Lou Y, Chen J, Yang Y, et al. PD-1 blockade enhances T-cell migration to tumors by elevating IFN-gamma inducible chemokines. Cancer Res. 2012 Oct 15;72(20):5209-18.
31. Yang J, Hu S, Shangguan J, Eresen A, Li Y, Pan L, et al. Dendritic cell immunotherapy induces anti-tumor effect in a transgenic mouse model of pancreatic ductal adenocarcinoma. Am J Cancer Res. 2019 Nov 1;9(11):2456-68.
32. Conzelmann M, Wagner AH, Hildebrandt A, Rodionova E, Hess M, Zota A, et al. IFN-gamma activated JAK1 shifts CD40-induced cytokine profiles in human antigen-presenting cells toward high IL-12p70 and low IL-10 production. Biochem Pharmacol. 2010 Dec 15;80(12):2074-86.
33. Cavallo F, Quaglino E, Cifaldi L, Di Carlo E, Andre A, Bernabei P, et al. Interleukin 12-activated lymphocytes influence tumor genetic programs. Cancer Res. 2001 Apr 15;61(8):3518-23.
34. Xue W, Li W, Zhang T, Li Z, Wang Y, Qiu Y, et al. Anti-PD1 up-regulates PD-L1 expression and inhibits T-cell lymphoma progression: possible involvement of an IFN-gamma-associated JAK-STAT pathway. Onco Targets Ther. 2019 Mar 19;12:2079-88.
35. Huen SC, Huynh L, Marlier A, Lee Y, Moeckel GW, Cantley LG. GM-CSF Promotes Macrophage Alternative Activation after Renal Ischemia/Reperfusion Injury. J Am Soc Nephrol. 2015 Jun;26(6):1334-45.
36. Galati G, Rovere P, Citterio G, Bondanza A, Scagliette U, Bucci E, et al. In vivo administration of GM-CSF promotes the clearance of apoptotic cells: effects on monocytes and polymorphonuclear leukocytes. J Leukoc Biol. 2000 Feb;67(2):174-82.
37. Swords DS, Firpo MA, Scaife CL, Mulvihill SJ. Biomarkers in pancreatic adenocarcinoma: current perspectives. Onco Targets Ther. 2016 Dec 9;9:7459-67.
38. Seppänen H, Juuti A, Mustonen H, Haapamäki C, Nordling S, Carpelan-Holmström M, et al. The Results of Pancreatic Resections and Long-Term Survival for Pancreatic Ductal Adenocarcinoma: A Single-Institution Experience. Scand J Surg. 2017 Mar;106(1):54-61.
39. Engle DD, Tiriac H, Rivera KD, Pommier A, Whalen S, Oni TE, et al. The glycan CA19-9 promotes pancreatitis and pancreatic cancer in mice. Science 2019;364:1156-62.
40. Pinette A, McMichael E, Courtney NB, Duggan M, Benner BN, Choueiry F, et al. An IL-15-based superantagonist ALT-803 enhances the NK cell response to cetuximab-treated squamous cell carcinoma of the head and neck. Cancer Immunol Immunother 2019;68:1379-89.

41. Beatty GL, Chiorean EG, Fishman MP, Saboury B, Teitelbaum UR, Sun W, et al. CD40 agonists alter tumor stroma and show efficacy against pancreatic carcinoma in mice and humans. Science. 2011 Mar 25;331(6024):1612-6.
42. Cui R, Yue W, Lattime EC, Stein MN, Xu Q, Tan XL. Targeting tumor-associated macrophages to combat pancreatic cancer. Oncotarget. 2016 Aug 2;7(31):50735-54.
43. Ino Y, Yamazaki-Itoh R, Shimada K, Iwasaki M, Kosuge T, Kanai Y, et al. Immune cell infiltration as an indicator of the immune microenvironment of pancreatic cancer. Br J Cancer. 2013 Mar 5;108(4):914-23.
44. Hu H, Hang JJ, Han T, Zhuo M, Jiao F, Wang LW. The M2 phenotype of tumor-associated macrophages in the stroma confers a poor prognosis in pancreatic cancer. Tumour Biol. 2016 Jul;37(7):8657-64.
45. Egberts JH, Cloosters V, Noack A, Schniewind B, Thon L, Klose S, et al. Anti-tumor necrosis factor therapy inhibits pancreatic tumor growth and metastasis. Cancer Res. 2008 Mar 1;68(5):1443-50.
46. Setrerrahmane S, Xu H. Tumor-related interleukins: old validated targets for new anti-cancer drug development. Mol Cancer. 2017 Sep 19;16(1):153,017-0721-9.
47. Gentile LF, Cuenca AG, Efron PA, Ang D, Bihorac A, McKinley BA, et al. Persistent inflammation and immunosuppression: a common syndrome and new horizon for surgical intensive care. J Trauma Acute Care Surg. 2012 Jun;72(6):1491-501.
48. Wang D, DuBois RN. Immunosuppression associated with chronic inflammation in the tumor microenvironment. Carcinogenesis. 2015 Oct;36(10):1085-93.
49. Javeed N, Gustafson MP, Dutta SK, Lin Y, Bamlet WR, Oberg AL, et al. Immunosuppressive CD14(+)HLA-DR(lo/neg) monocytes are elevated in pancreatic cancer and "primed" by tumor-derived exosomes. Oncoimmunology. 2016 Nov 2;6(1):e1252013.

Supplementary

Supplementary Figure 1.

Supplementary Table 1.

	Patient (n=6)			Control (n=5)			
Marker	Median (RFU)	Q1 (RFU)	Q3 (RFU)	Median (RFU)	Q1 (RFU)	Q3 (RFU)	p=
CD14	123.47	110.91	135.97	110.62	108.44	136.26	0.931
CD204	64.61	46.98	73.65	63.21	48.70	63.78	0.931
CD209	14.15	9.65	25.03	11.86	7.23	15.40	0.537
CD163	58.11	48.26	82.79	60.43	44.11	61.53	0.792
CD86	51.07	33.08	109.41	41.42	27.38	48.70	0.429

No initial difference could be found in the expression of CD markers on monocytes from pancreatic cancer patients and healthy controls.

Supplementary Table 2.

		CA19-9			CEA	
Molecule	**Stimulation**	**r (95% CI)**	**p**		**r (95% CI)**	**p**
pSTAT1	Constitutive	-0.348 (-0.671 to 0.087)	0.113		-0.079 (-0.484 to 0.355)	0.728
	IL-6	0.133 (-0.306 to 0.525)	0.556		0.152 (-0.288 to 0.539)	0.500
	IFN-γ	**-0.475 (-0,747 to -0.067)**	**0.025**		0.169 (-0.272 to 0.551)	0.452
pSTAT2	Constitutive	**0.612 (0.257 to 0.822)**	**0.002**		-0.124 (-0.518 to 0.314)	0.583
pSTAT3 (pS727)	Constitutive	0.018 (-0.407 to 0.436)	0.938		0.160 (-0.280 to 0.545)	0.476
	IL-6	0.207 (-0.235 to 0.578)	0.355		-0.319 (-0.653 to 0.119)	0.148
pSTAT3 (pY705)	Constitutive	0.082 (-0.352 to 0.487)	0.717		0.161 (-0,280 to 0.546)	0.474
	IL-6	0.318 (-0.120 to 0.652)	0.150		-0.415 (-0.712 to 0.008)	0.055
pSTAT4	Constitutive	0.215 (-0.227 to 0.584)	0.336		0.064 (-0.367 to 0.437)	0.776
pSTAT5	Constitutive	**0.492 (0.077 to 0.762)**	**0.023**		-0.152 (-0.548 to 0.299)	0.511
	GM-CSF + IL-4	0.137 (-0.314 to 0.537)	0.555		0.169 (-0.284 to 0.560)	0.464
pSTAT6	Constitutive	-0.018 (-0.446 to 0.417)	0.940		-0.264 (-0.624 to 0.190)	0.248
	GM-CSF + IL-4	0.154 (-0.297 to 0.549)	0.505		-0.243 (-0.611 to 0.211)	0.289
pNF-κB	Constitutive	-0.297 (-0.646 to 0.154)	0.191		0.145 (-0.305 to 0.543)	0.529
	TNF + LPS	-0.135 (-0.536 to 0.315)	0.559		0.022 (-0.414 to 0.449)	0.924
pAkt	Constitutive	0.148 (-0.303 to 0.545)	0.523		0.069 (-0.350 to 0.507)	0.679
	TNF + LPS	0.092 (-0.354 to 0.503)	0.693		-0.014 (-0.443 to 0.420)	0.951

CA19-9 level showed a positive correlation with constitutive STAT2 and STAT5 phosphorylation levels, and a negative correlation with IFN-γ -induced STAT2 and STAT1 phosphorylation.

Supplementary Figure Legends:

Figure S6.

Flow cytometric determination of CD14+ monocyte HLA-DR expression. Monocytes were identified among all leucocytes based on CD14-FITC positivity (A) and subsequently on forward/side scatter characteristics (B). A gate (HLA-DR+) was set to exclude the PE signal from the isotype control (C, dashed line) and used to measure the proportion of PE positive events on the HLA-DR-PE-stained sample (C, solid line).

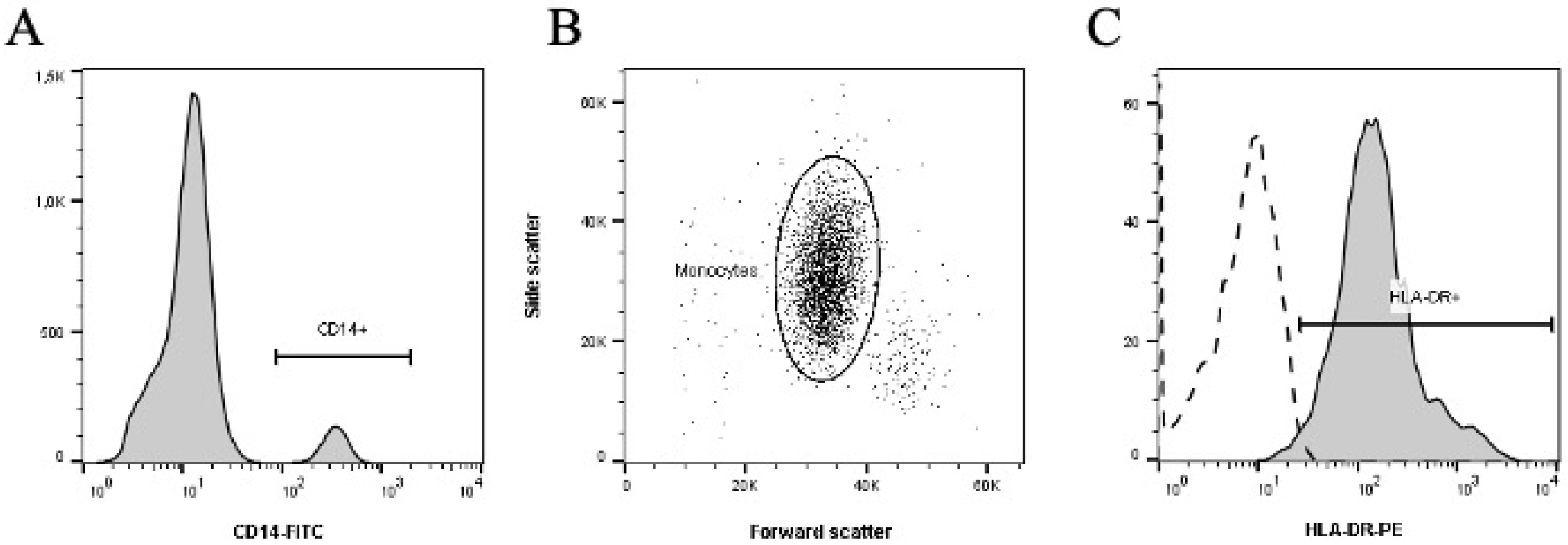
A
1,5K
1,0K
500
0
CD14+
10^0
10^1
10^2
10^3
10^4
CD14-FITC
B
60K
40K
20K
0
Side scatter
Monocytes
0
20K
40K
60K
Forward scatter
C
60
40
20
0
HLA-DR+
10^0
10^1
10^2
10^3
10^4
HLA-DR-PE

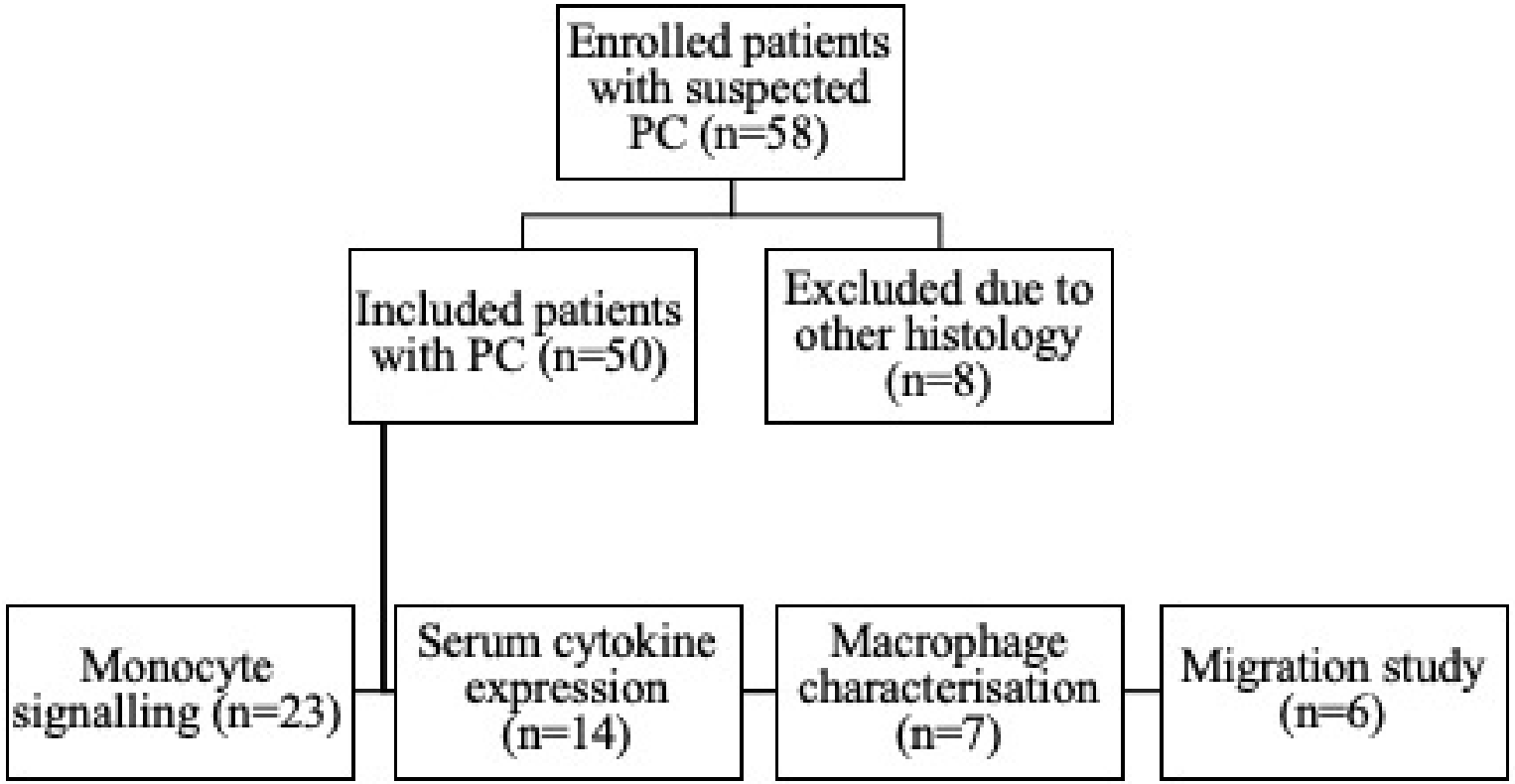
Enrolled patients with suspected PC (n=58)
Included patients with PC (n=50)
Excluded due to other histology (n=8)
Monocyte signalling (n=23)
Serum cytokine expression (n=14)
Macrophage characterisation (n=7)
Migration study (n=6)

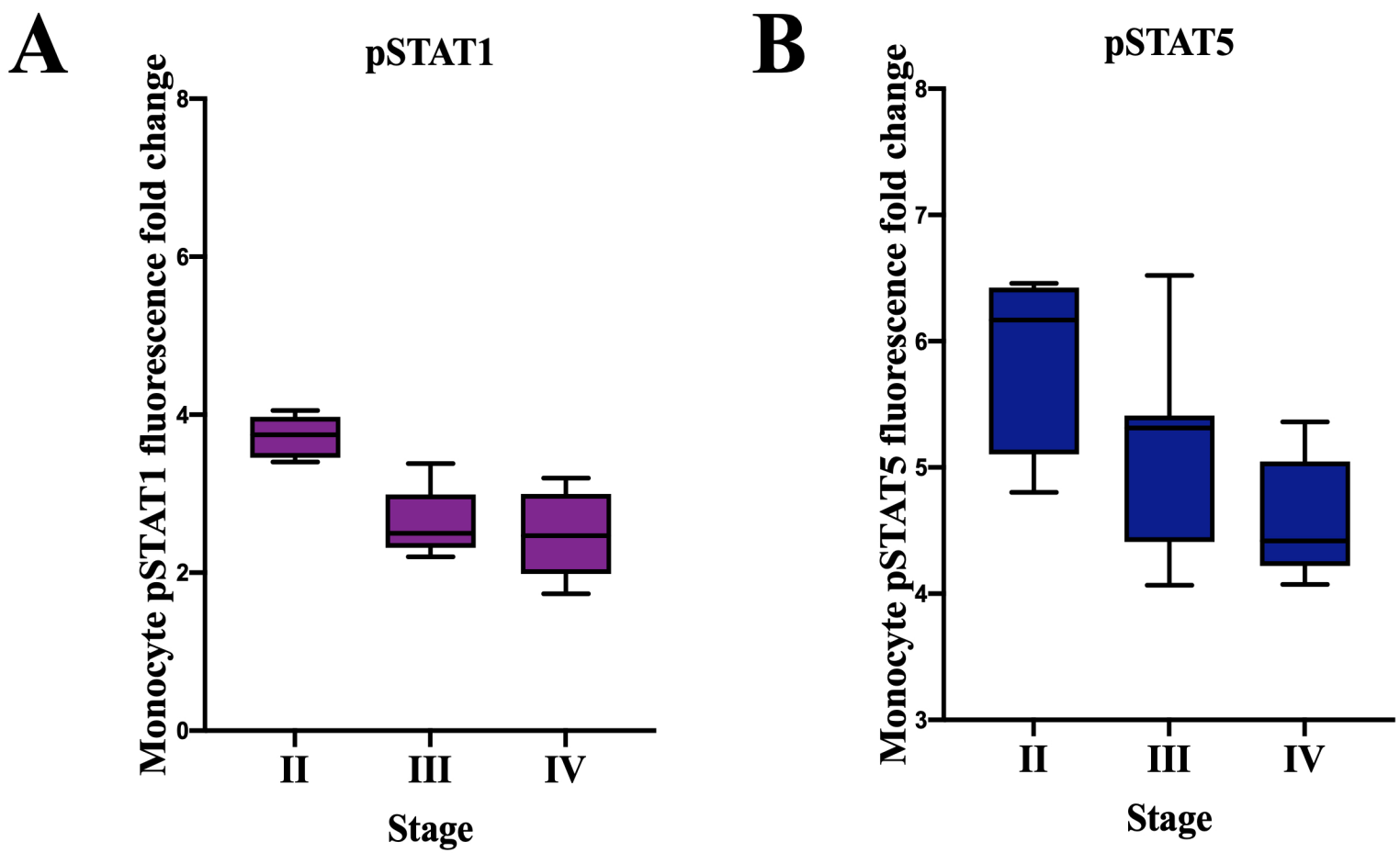
A
pSTAT1
Monocyte pSTAT1 fluorescence fold change
0
2
4
6
8
II
III
IV
Stage
B
pSTAT5
Monocyte pSTAT5 fluorescence fold change
3
4
5
6
7
8
II
III
IV
Stage

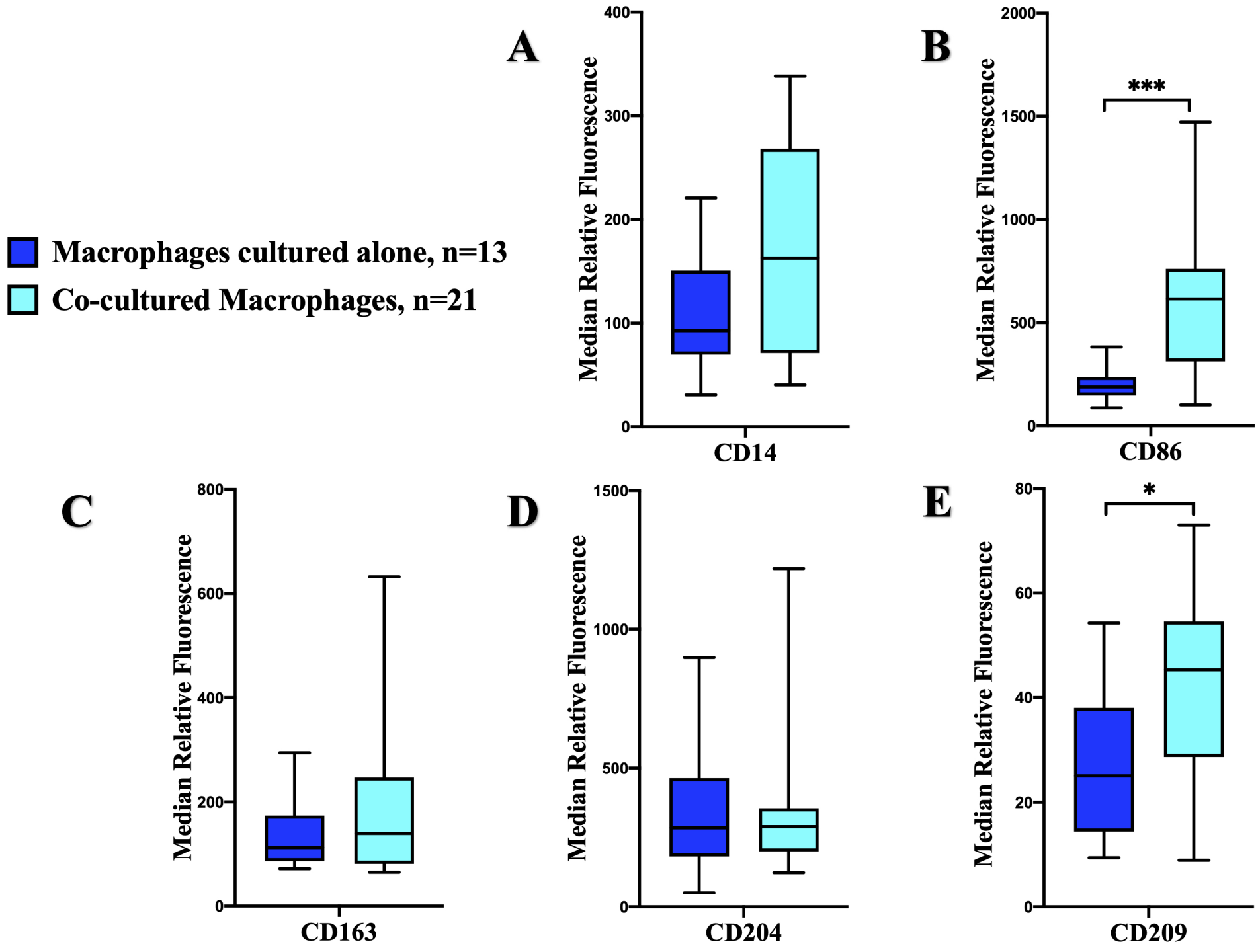
Macrophages cultured alone, n=13
Co-cultured Macrophages, n=21
A
Median Relative Fluorescence
400
300
200
100
0
CD14
B
Median Relative Fluorescence
2000
1500
1000
500
0
***
CD86
C
Median Relative Fluorescence
800
600
400
200
0
CD163
D
Median Relative Fluorescence
1500
1000
500
0
CD204
E
Median Relative Fluorescence
80
60
40
20
0
*
CD209

Macrophages cultured alone, n=6-7

Macrophages co-cultured with MIA PaCa-2, n=6–7

Macrophages co-cultured with HPAF-II, n= 4

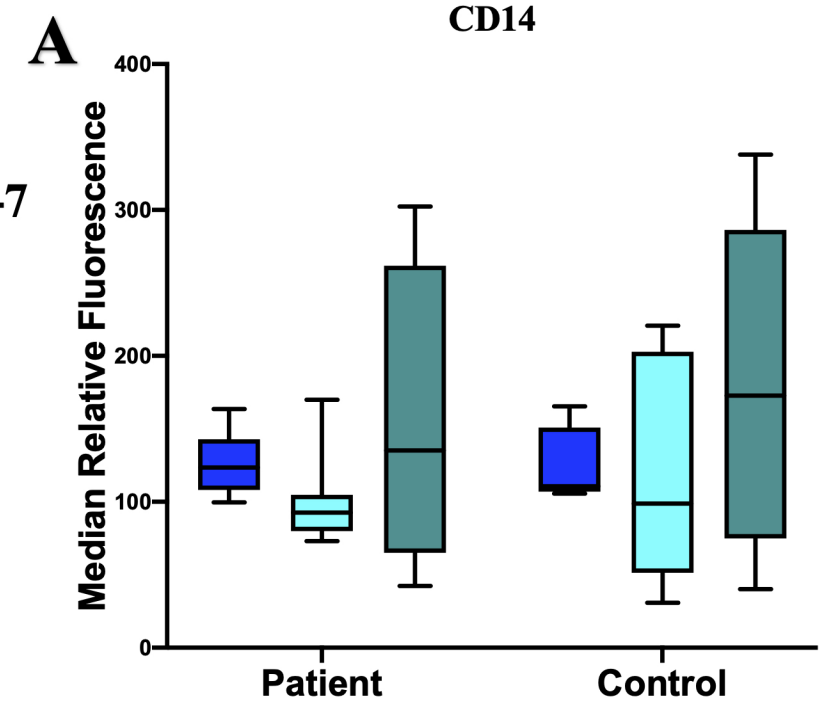

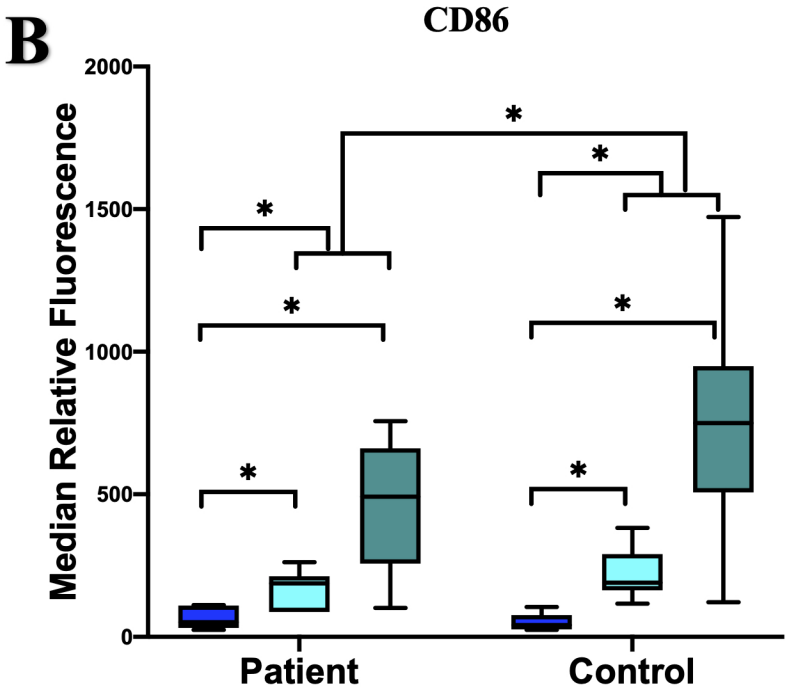

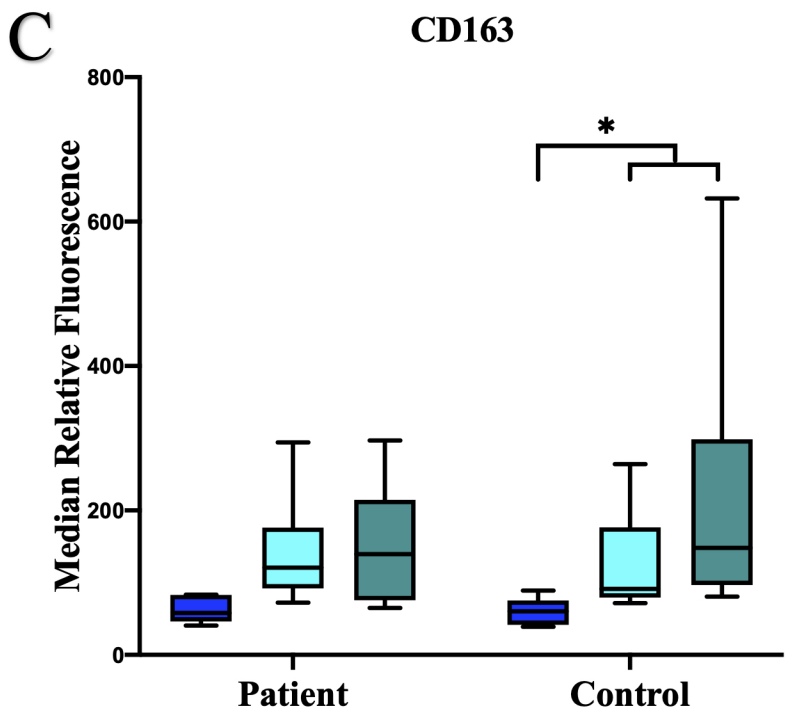

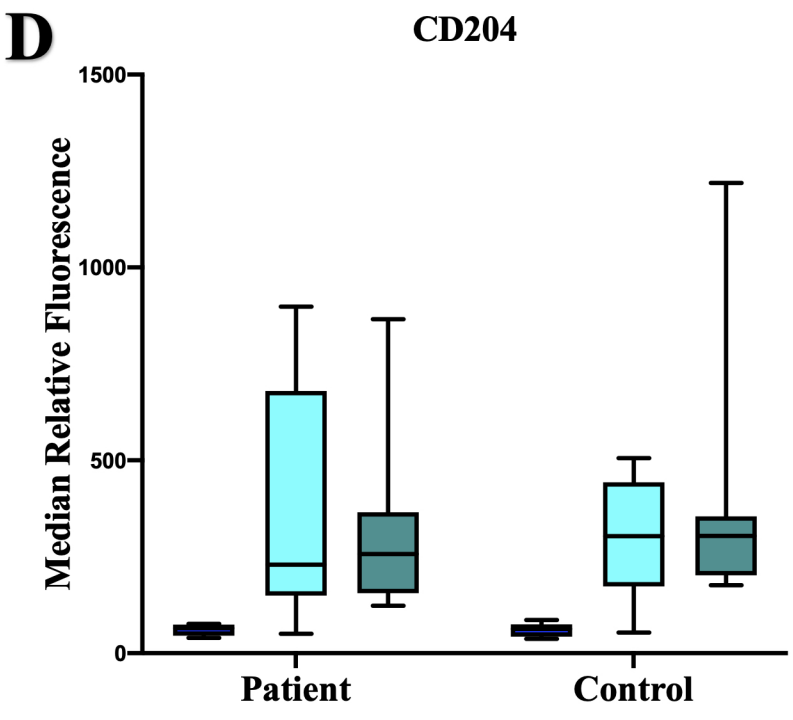

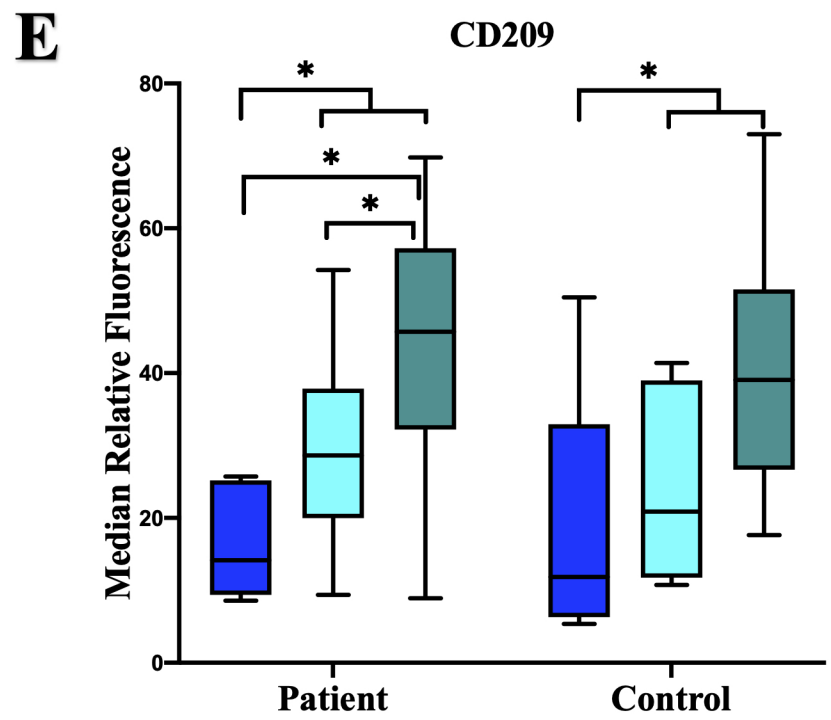

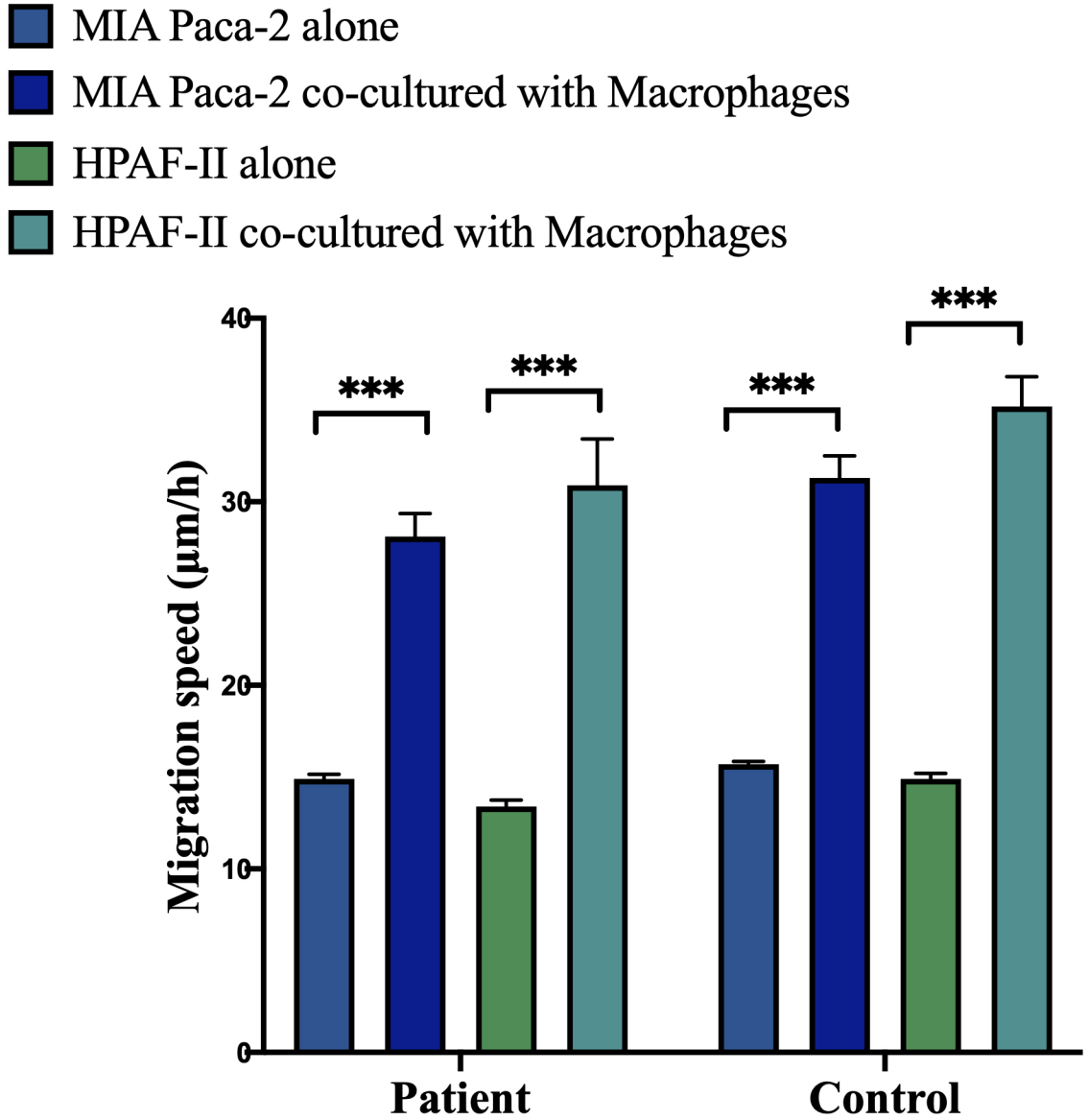
MIA Paca-2 alone
MIA Paca-2 co-cultured with Macrophages
HPAF-II alone
HPAF-II co-cultured with Macrophages
Migration speed (μm/h)
0
10
20
30
40
***
***
***
***
Patient
Control

Supplementary Table 1.

	Patient (n=6)			Control (n=5)			
Marker	Median (RFU)	Q1 (RFU)	Q3 (RFU)	Median (RFU)	Q1 (RFU)	Q3 (RFU)	p=
CD14	123.47	110.91	135.97	110.62	108.44	136.26	0.931
CD204	64.61	46.98	73.65	63.21	48.70	63.78	0.931
CD209	14.15	9.65	25.03	11.86	7.23	15.40	0.537
CD163	58.11	48.26	82.79	60.43	44.11	61.53	0.792
CD86	51.07	33.08	109.41	41.42	27.38	48.70	0.429

Supplementary table 2.

		CA19-9		CEA	
Molecule	**Stimulation**	**r (95% CI)**	**p**	**r (95% CI)**	**p**
pSTAT1	Constitutive	-0.348 (-0.671 to 0.087)	0.113	-0.079 (-0.484 to 0.355)	0.728
	IL-6	0.133 (-0.306 to 0.525)	0.556	0.152 (-0.288 to 0.539)	0.500
	IFN-γ	**-0.475 (-0,747 to -0.067)**	**0.025**	0.169 (-0.272 to 0.551)	0.452
pSTAT2	Constitutive	**0.612 (0.257 to 0.822)**	**0.002**	-0.124 (-0.518 to 0.314)	0.583
	IFN-α	**-0.581 (-0.805 to -0.211)**	**0.005**	-0.183 (-0.561 to 0.259)	0.415
pSTAT3 (pS727)	Constitutive	0.018 (-0.407 to 0.436)	0.938	0.160 (-0.280 to 0.545)	0.476
	IL-6	0.207 (-0.235 to 0.578)	0.355	-0.319 (-0.653 to 0.119)	0.148
pSTAT3 (pY705)	Constitutive	0.082 (-0.352 to 0.487)	0.717	0.161 (-0,280 to 0.546)	0.474
	IL-6	0.318 (-0.120 to 0.652)	0.150	-0.415 (-0.712 to 0.008)	0.055
pSTAT4	Constitutive	0.215 (-0.227 to 0.584)	0.336	0.064 (-0.367 to 0.437)	0.776
	IFN-α	-0.259 (-0.614 to 0.183)	0.245	-0.314 (-0.650 to 0.124)	0.155
pSTAT5	Constitutive	**0.492 (0.077 to 0.762)**	**0.023**	-0.152 (-0.548 to 0.299)	0.511
	GM-CSF + IL-4	0.137 (-0.314 to 0.537)	0.555	0.169 (-0.284 to 0.560)	0.464
pSTAT6	Constitutive	-0.018 (-0.446 to 0.417)	0.940	-0.264 (-0.624 to 0.190)	0.248
	GM-CSF + IL-4	0.154 (-0.297 to 0.549)	0.505	-0.243 (-0.611 to 0.211)	0.289
pNF-κB	Constitutive	-0.297 (-0.646 to 0.154)	0.191	0.145 (-0.305 to 0.543)	0.529
	TNF + LPS	-0.135 (-0.536 to 0.315)	0.559	0.022 (-0.414 to 0.449)	0.924
pAkt	Constitutive	0.148 (-0.303 to 0.545)	0.523	0.069 (-0.350 to 0.507)	0.679
	TNF + LPS	0.092 (-0.354 to 0.503)	0.693	-0.014 (-0.443 to 0.420)	0.951

Table 1.

Molecule	Stimulation	Patients Mean (95% CI)	Controls Mean (95% CI)	p
pSTAT1	Constitutive	1.06 (1.00 - 1.12)	0.96 (0.92 - 1.01)	**0.031**
	IL-6	1.35 (1.25 - 1.47)	1.40 (1.30 - 1.50)	0.70
	IFN-γ	3.04 (2.65 - 3.55)	3.05 (2.58 - 3.63)	0.99
pSTAT2	Constitutive	4.36 (3.99 - 4.74)	3.67 (3.21 - 4.13)	**0.031**
	IFN-α	1.22 (1.17 - 1.27)	1.29 (1.23 - 1.34)	0.084
pSTAT3 (pS727)	Constitutive	2.13 (1.92 - 2.35)	1.83 (1.65 - 2.04)	**0.031**
	IL-6	2.32 (2.15 - 2.52)	2.44 (2.26 - 2.67)	0.37
pSTAT3 (pY705)	Constitutive	1.86 (1.73 - 2.07)	1.47 (1.33 - 1.64)	**<0.001**
	IL-6	5.7 (5.30 - 6.21)	5.86 (5.12 - 6.72)	0.97
pSTAT4	Constitutive	1.66 (1.58 - 1.75)	1.56 (1.40 - 1.74)	0.20
	IFN-α	1.04 (1.01 - 1.06)	1.04 (1.02 - 1.06)	0.71
pSTAT5	Constitutive	2.97 (2.73 - 3.28)	2.64 (2.33 - 2.94)	0.088
	GM-CSF + IL-4	5.10 (4.75 - 5.46)	5.95 (5.46 - 6.47)	**0.006**
pSTAT6	Constitutive	1.01 (0.96 - 1.06)	0.91 (0.86 - 0.96)	**0.018**
	GM-CSF + IL-4	1.35 (1.25 - 1.47)	1.40 (1.30 - 1.50)	0.19
pNF-κB	Constitutive	1.25 (1.18 - 1.32)	1.16 (1.08 - 1.23)	0.32
	TNF + LPS	2.31 (2.13 - 2.51)	2.83 (2.59 - 3.09)	**0.004**
pAkt	Constitutive	1.99 (1.81 - 2.18)	2.00 (1.69 - 2.32)	0.90
	TNF + LPS	2.04 (1.93 - 2.19)	2.17 (2.00 - 2.43)	0.28

Table 2.

Cytokine	Patient Median (IQR)	Control Median (IQR)	p
IFN-y	1.59 (0.96)	1.22 (0.67)	0.397
IL-1α	1.96 (14.58)	0.59 (1.92)	0.312
IL-1β	18.65 (22.6)	8.75 (0.00)	**0.041**
IL-1ra	55.33 (68.04)	34.73 (14.72)	0.051
IL-6	3.32 (1.51)	2.21 (0.82)	**0.041**
IL-8	3.28 (2.73)	3.28 (0.00)	0.659
IL-10	12.21 (7.79)	4.57 (0.00)	**0.002**
IL-23	58.45 (40.81)	47.91 (53.28)	0.750
MCP-1	68.54 (41.22)	71.38 (19.92)	0.602
RANTES	1868.90 (917.57)	1182.10 (580.30)	**0.005**
TNF	15.41 (9.05)	6.89 (0.74)	**0.003**

Supplementary Table 1.

	Patient (n=6)			Control (n=5)			
Marker	Median (RFU)	Q1 (RFU)	Q3 (RFU)	Median (RFU)	Q1 (RFU)	Q3 (RFU)	p=
CD14	123.47	110.91	135.97	110.62	108.44	136.26	0.931
CD204	64.61	46.98	73.65	63.21	48.70	63.78	0.931
CD209	14.15	9.65	25.03	11.86	7.23	15.40	0.537
CD163	58.11	48.26	82.79	60.43	44.11	61.53	0.792
CD86	51.07	33.08	109.41	41.42	27.38	48.70	0.429

Supplementary table 2.

		CA19-9		CEA	
Molecule	**Stimulation**	**r (95% CI)**	**p**	**r (95% CI)**	**p**
pSTAT1	Constitutive	-0.348 (-0.671 to 0.087)	0.113	-0.079 (-0.484 to 0.355)	0.728
	IL-6	0.133 (-0.306 to 0.525)	0.556	0.152 (-0.288 to 0.539)	0.500
	IFN-γ	**-0.475 (-0,747 to -0.067)**	**0.025**	0.169 (-0.272 to 0.551)	0.452
pSTAT2	Constitutive	**0.612 (0.257 to 0.822)**	**0.002**	-0.124 (-0.518 to 0.314)	0.583
	IFN-α	**-0.581 (-0.805 to -0.211)**	**0.005**	-0.183 (-0.561 to 0.259)	0.415
pSTAT3 (pS727)	Constitutive	0.018 (-0.407 to 0.436)	0.938	0.160 (-0.280 to 0.545)	0.476
	IL-6	0.207 (-0.235 to 0.578)	0.355	-0.319 (-0.653 to 0.119)	0.148
pSTAT3 (pY705)	Constitutive	0.082 (-0.352 to 0.487)	0.717	0.161 (-0,280 to 0.546)	0.474
	IL-6	0.318 (-0.120 to 0.652)	0.150	-0.415 (-0.712 to 0.008)	0.055
pSTAT4	Constitutive	0.215 (-0.227 to 0.584)	0.336	0.064 (-0.367 to 0.437)	0.776
	IFN-α	-0.259 (-0.614 to 0.183)	0.245	-0.314 (-0.650 to 0.124)	0.155
pSTAT5	Constitutive	**0.492 (0.077 to 0.762)**	**0.023**	-0.152 (-0.548 to 0.299)	0.511
	GM-CSF + IL-4	0.137 (-0.314 to 0.537)	0.555	0.169 (-0.284 to 0.560)	0.464
pSTAT6	Constitutive	-0.018 (-0.446 to 0.417)	0.940	-0.264 (-0.624 to 0.190)	0.248
	GM-CSF + IL-4	0.154 (-0.297 to 0.549)	0.505	-0.243 (-0.611 to 0.211)	0.289
pNF-κB	Constitutive	-0.297 (-0.646 to 0.154)	0.191	0.145 (-0.305 to 0.543)	0.529
	TNF + LPS	-0.135 (-0.536 to 0.315)	0.559	0.022 (-0.414 to 0.449)	0.924
pAkt	Constitutive	0.148 (-0.303 to 0.545)	0.523	0.069 (-0.350 to 0.507)	0.679
	TNF + LPS	0.092 (-0.354 to 0.503)	0.693	-0.014 (-0.443 to 0.420)	0.951